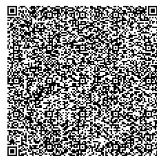

Mapana – Journal of Sciences
2026, Vol. 25, No. 2, *1-20*
ISSN 0975-3303 | https://doi.org/10.12723/mjs.77.1

Electrical Resistance Modulation in Silver Oxide Thin Films as a Function of Thickness

Shivakumar Siddanna*, Devidas G. B.*, S. M. Hanagodimath†, Omnath Patil†

Abstract

Silver oxide thin films have been deposited on engraved fluorine-doped tin oxide (FTO) glass substrates using the radio-frequency (RF) sputtering technique. RF sputtering was selected for its ability to produce uniform, high-quality thin films with good adhesion to the substrate. After deposition, the films have been subjected to post–deposition annealing at 200°C for 2 hours to improve their structural stability and electrical properties. Thicknesses of deposited films vary from ~42-~ 660 nm and was precisely measured utilizing 3Dnon contact optical profiler. The electrical characteristics of Ag_2O thin films have been examined through current–voltage (I-V) measurements performed at room temperature. Results indicate that the electrical resistivity decreased with increasing thin-film thickness due to improved continuity, then increased at higher thicknesses, which can be attributed to changes in grain structure, defect density, and carrier transport mechanisms. Electrical resistance measurements were performed using the Vander Pauw method, ensuring accurate resistivity measurements for thin-film samples. Structural analysis of deposited films was conducted using X-ray diffraction (XRD), which provided insights into the crystallographic phases and orientations of the Silver Oxide films. Additionally, surface morphology and microstructural properties have been studied using field-emission scanning electron microscopy (FESEM), providing information on grain size, surface uniformity, and film continuity.

Keywords: Silver oxide, RF sputtering, Annealing, XRD and FESEM.

---

* Dept of Physics Kuvempu University Shankaraghatta, Shimogga, Karnataka, India; sbhairamadagi@gmail.com, devidasgb02@gmail.com

† Dept of Physics, Gulbarga University, Kalaburagi, Karnataka, India; smhmath@rediffmail.com, omnathpatil@gmail.com

1. Introduction

Molecular technology operates at the nanoscale, where materials usually exhibit isolated and strengthened properties, emerging from high "surface area to volume ratios (SA/V)" and quantum effects. These include chemical reactivity, improved electrical conductivity, novel magnetic and optical behaviors, and superior mechanical strength. Among the numerous types of nanomaterials, silver oxide thin films have attracted significant attention, especially when deposited on fluorine-doped tin oxide (FTO) glass substrates. Band gap of Ag_2O is a positive charge semiconductor with band gap varies from 1.2 - 3.4 eV, its notable optical and electrical characteristics' make it a promising candidate for application in photovoltaics photo catalysis, sensor rechargeable batteries etc. however, limitations such as its relatively wide band gap and susceptibility to thermal decomposition, which can generate light scattering centers and microscopic surface defects, pose challenge for practical application. To address these issues, researchers have explored various deposition techniques, including spray pyrolysis, spin coating, e-beam evaporation, pulsed laser deposition (PLD), and both thermal, DC and RF sputtering. RF sputtering provides highly energetic plasma conditions favourable for uniform thin-film growth. Nano-crystalline Ag_2O thin films fabricated through this method are of considerable interest for optical and biological micro devices, nanoscale electronics, and other advanced technologies. Its band gap was determined to be approximately **2.2 eV** [1-3]. Nevertheless, comparatively few studies have systematically examined the influence of electrical, structural, film thickness and optical characteristics of RF-sputtered Ag_2O thin films [4–8].

In this research work, Ag_2O nanofilms were successfully grown by using RF magnetron sputtering. The electrical resistance was measured by the Van der Pauw method with a four-probe configuration to ensure accurate assessment of in-plane properties. Film thickness fluctuates from 42 nm to 660nm, which was determined using a 3D non-contact optical Profilometer. To elucidate the thickness–dependent behaviour, detailed analyses of electrical conductivity, structural evolution, and microstructural characteristics were conducted. XRD studies with the help of the Rigaku Smart Lab system were employed to confirm crystallinity, FESEM was utilised to measure grain size, and surface morphology and uniformity of the film were determined.

Theoretical background

The Vander pauw method was first discovered by L.J Vander pauw in 1958[9] as reliable and accurate techniques to determine the hall coefficient and resistivity of thin films, flat samples with arbitrary shapes. This

technique was very popular and widely adopted in nano films, material science, solid state physics and semiconductor research for characterizing electrical characteristics of nano thin films.

To successfully apply Vander pauw technique, the following five essential criteria must be satisfied [10];

4. The sample must have uniform thickness and a smooth surface.
5. The samples should have restricted gaps or be free of isolated holes.
6. The material should be **homogeneous** and **isotropic** in nature.
7. All **4 electrical contacts** should be placed precisely at **the edges of the** sample.
8. Each contact should be very small or in a dot, ideally at least one order of magnitude smaller than the sample's overall dimensions.

When these conditions are met, the Vander pauw technique enables precise evaluation for the electrical properties of the materials, even for irregularly shaped samples, making it particularly useful for thin films characterization.

Condition for the sample preparation for I-V measurements

- The thickness of the sample must be much less than the sample’s length and breadth.
- There must be no isolated voids within the samples. The samples should be symmetrical.
- Measurements require four ohmic connections (silver paste) to be painted on the sample.
- Certain conditions for their placement need to be met: They must be infinitely small. They must be on the boundary of the sample.

Square or rectangle: contact at the corners

Four-probe schematic diagram for electrical measurements

Measurement definitions

The current 12(I) position is measured in amperes (A) and represents a Positive direct current flowing from contact 1 to contact 2.

The voltage 34 (V) is a direct current voltage determined in volts (V), measured between contacts 3 and 4 in the absence of an external magnetic field.

- Resistivity (rho) is measured in ohms per meter (Ω · m).
- Measuring the sample thickness (t) is in meters (M).
- The R_S sheet resistance is measured in ohm (Ω).

Measurement of the resistivity:

$\rho = R_S \times (t)$ using this formula, to calculate the sample's average resistivity.

Here, R_S is the sheet resistance, and (t) is the thickness of the sample.

2. Experimental Methods

2.1. Substrate cleaning process

Prior to deposition, FTO-glazed glass substrates underwent a rigorous multi-step cleaning process to remove organic and inorganic contaminants that could compromise adhesion of the film or uniformity. The substrates were first immersed in chromic acid **(H_2CrO_4 - 52% of pure)** solution to, oxidize and remove organic residues, followed by treatment with weak acid i.e. hydrofluoric acid **(HF - 48% of pure)** to etch surface oxides and dislodge undesirable materials. Rinsing with deionised (DI) water was performed after each acid treatment to remove residual substances. To further eliminate greasy substances and microscopic debris, substrates were subjected to ultrasonic cleaning in DI water at 50 °C, where cavitation aided in removing particles. Further chromic acid treatment was applied to ensure complete decontamination. The cleaned substrate was dried with a hot-air blower in a dust-free, clean room, and finally swabbed with ethanol- or acetone-soaked lint-free tissues to remove residual moisture. It enhances surface activation. This comprehensive cleaning procedure ensured a perfect substrate surface, enabling uniform deposition and strong adhesion of silver oxide thin films.

2.2. Thin film deposition using RF magnetron sputtering:

Silver oxide thin films were deposited on pre-etched FTO glass substrates using RF magnetron sputtering. This process has been employed for its ability to generate uniform, dense and adherent films having controlled stoichiometry. A 99.99% pure silver target served as the sputtering source, and the substrate (1x1) cm^2 was positioned 75 cm from the target. The Sputtering chamber has been evacuated to a base pressure of 4 × 10^-6 mbar

using a rotary pump coupled with a diffusion pump to ensure a contamination-free environment. Argon was employed as the inert sputtering gas, while oxygen was introduced as a reactive gas to facilitate in situ formation of silver oxide. Gas flow rates and partial pressures were finely regulated using precision needle valves. Deposition has been conducted at room temperature with an applied RF power of 100 W. The working pressure was maintained at 4 Pa, with an oxygen partial pressure of 2Pa. These optimized conditions favored the growth of stoichiometric silver oxide films while minimizing the formation of non-stoichiometric phases[11].

2.3. Measurement of film thickness:

The Silver Oxide films thickness can be identified by using two different methods, which are as follows:

1. **Gravimetric method**: In this method, the film thickness can be calculated indirectly based on the weight of the deposited material and also the known density of silver oxide, along with the deposition time and substrate area. This gravimetric approach provides a useful cross verification for the thickness measurements, especially when a large area uniformity is assumed.
2. **Non-contact optical profiler**: a three-dimensional optical profiler was utilised for determining the film's thickness directly. This technique provides high-resolution surface proofing without damaging the sample, allowing the accurate thickness determination over a localised area.

2.4. Post-deposition annealing

All the deposited silver oxide thin films have been subjected to a post-deposition annealing treatment for two hours in air at 200 °C. To remove impurities in the film, we have chosen 200 °C as the annealing temperature. If we have raised the temperature in the annealing process, the film may crack and later the continuity will be broken. This thermal treatment was performed to increase the crystallinity and structural stability of the films, which promotes phase formation and removes any defects or residual stress introduced during sputtering. Annealing facilitates grain growth, which can affect the electrical and morphological properties of thin films [12].

2.5. Electrical characterization

Electrical resistance of annealed silver oxide thin films was measured using the Vander pauw method that is appropriate to identify sheet resistance of

thin, uniform and arbitrarily shaped conducting films. This four probe method allows for error free resistance measurement by eliminating contact resistance effects. It provides that the film is uniform in thickness; the contacts are ohmic and placed at the corners or edges of the sample.

2.6. Structural and morphological characterization

A Rigaku SmartLab diffractometer operating at 40kV and 30mA has been utilised for XRD analysis, utilising CuKb radiation as the X-ray source, in order to evaluate the crystallographic structure of the produced thin films. The diffraction pattern was recorded in the 2 theta range an angles of 15 to 60, enabling identification of the crystalline phase, lattice parameters, and preferred orientation of silver oxide thin films. Film surface topography and morphology were identified by using FESEM. This technique offers high-resolution images of film surface. It allowing observation of grain structure, film uniformity, surface roughness. FESEM analysis is the crucial to correlate surface features with electrical and structural features of films.

3. Results and Discussions

3.1. Non contact optical profiler

Surface morphology as well as thickness of silver oxide thin films has been investigated utilizing 3D non-contact optical profiler, which enables high resolution three dimensional surface characterizations without damaging the sample. In addition to thickness determination, the profiler provided quantitative information on surface roughness and topographical uniformity. Film thickness was determined by using step height method. Copper strips were placed on the FTO substrate prior to deposition, leaving a masked region free of film. After sputtering, the mask was removed, creating a sharp step edge between coated and uncoated areas. The optical profiler scan across this step provided precise thickness measurements. It represents scan images are shown in Figures 1a and 1b, corresponding to two deposition conditions. The measured film thickness which is merely 326 nm and 660 nm, confirming controlled deposition through RF magnetron sputtering and demonstrating consistency between sputtering parameters and film growth rate. The profiler analysis further indicated smooth surface morphology with low roughness values and minimal irregularities, reflecting uniform film growth and strong adhesion to substrate. Such smoothness is beneficial for the applications requiring optically transparent or electronically homogeneous thin films, including photovoltaic and gas sensors devices.

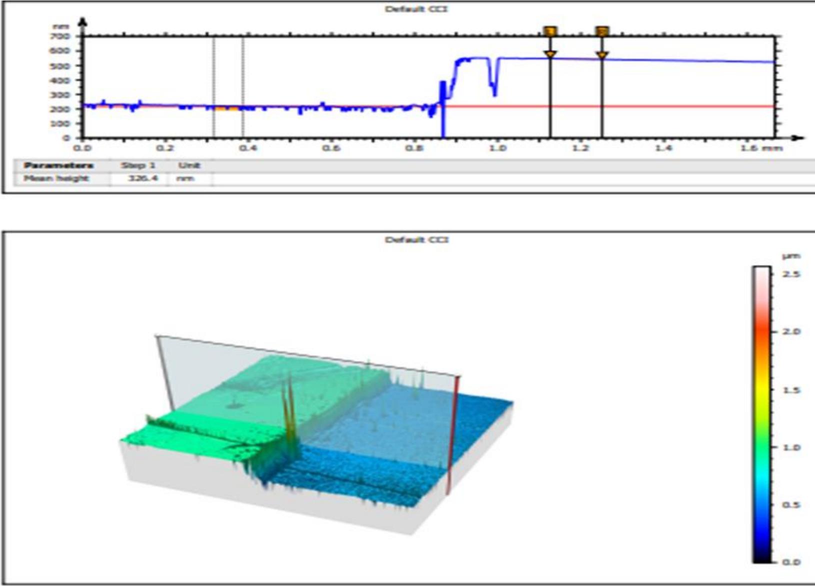

Figure 1a: Non contact optical profiler silver oxide film thickness of 326 nm

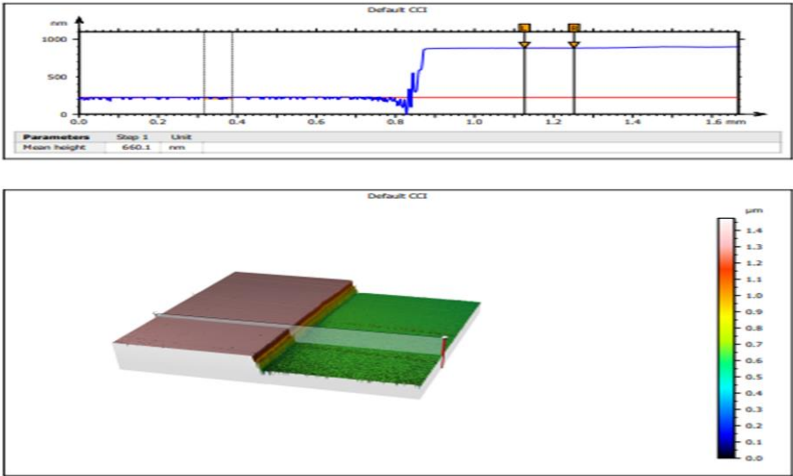

Figure 1 b: Non-contact optical profiler silver oxide film thickness 660 nm

3.2. Analysis of Current- Voltage (I-V) by using the Vander Pauw method.

Electrical measurement of silver oxide thin films has been performed at room temperature to analyse their conductivity behaviour. Current vs.

Voltage (I-V) characteristics were obtained by applying a bias voltage across the film and measuring the resulting current. These measurements provide insight into the electrical transport properties and the nature of conduction in the thin film.

Figure 2 displays the I-V curves for the silver oxide film with a thickness of 42 nm. The graph displays a nonlinear behavior in the low-voltage region, where the current initially increases with increasing voltage, indicating ohmic conduction. However, beyond a bias voltage of nearly 0.4V, the increase in current becomes relatively slow, showing a near-saturation behaviour. This region suggests a transition to space-charge-limited conduction (SCLC) or the presence of trap states that influence charge transport. One linear fit has been utilized to data to approximate conductance, and the slope of the fitted line yielded a conductance value of $1.53 \times 10-^{10}$mho [13].

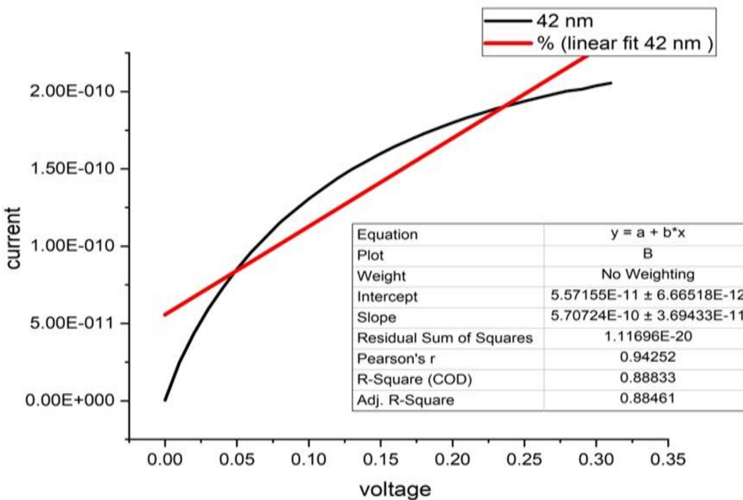

Figure 2: I –V Characterstics silver oxide film by using the Vander pauwmethod at 42 nm

In contrast, Figure 3 represents the I-V characteristics for a film with 72nm thickness. This graph exhibits a linear relationship over the entire measured voltage range, suggesting ohmic conduction behaviour without significant trap-limited or saturation effects. The calculated conductance from the slope of the linear fit is 2.25×10^{-9} mho, indicating a higher conductivity compared to the thinner 42 nm film. This increase in conductance with film thickness may be attributed to improved crystallinity, enhanced grain conductivity, or reduced defect density in thicker films.

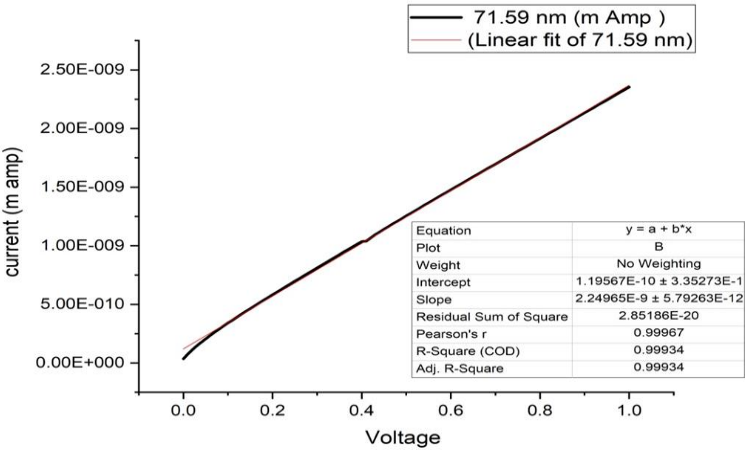

Figure 3: I –V Characterstics silver oxide film by using vander pauw method at 72 nm

These trends are consistent with previous findings reported for silver oxide[14] and zinc oxide [15] thin films, where film thickness and structural quality play a vital role in identifying electrical properties. Observed variation in the I-V behaviour between the two thicknesses highlights the importance of optimising deposition parameters to achieve the desired electronic performance in thin-film devices.

3.3. Measurement of sheet resistance

The electrical resistivity and sheet resistance of silver oxide thin films have been assessed using the van der Pauw four-point probe configuration. This method is well-suited for thin films of arbitrary shape, provided they are continuous, homogeneous, and of uniform thickness. The I-V curves obtained for all samples (Fig.4-6) exhibited linear behaviour, confirming ohmic contacts among films and electrodes in the absence of interfacial barriers. This linearity, along with negligible voltage variation across the four corners, indicates uniform electrical conductivity and consistent film thickness across the samples, validating the reliability of the derived sheet resistance values. A clear dependence of sheet resistance on film thickness was observed. Thinner films exhibited higher resistance, likely due to increased grain boundary scattering and a greater density of defects and discontinuities. Conversely, thicker films showed lower resistance,which can be attributed to improved crystallinity and reduced scattering centres that facilitate charge transport. These trends are consistent with earlier reports on silver oxide thin films [16], the reproducibility of the I-V curves underscores the reliability of the vander pauw measurements.

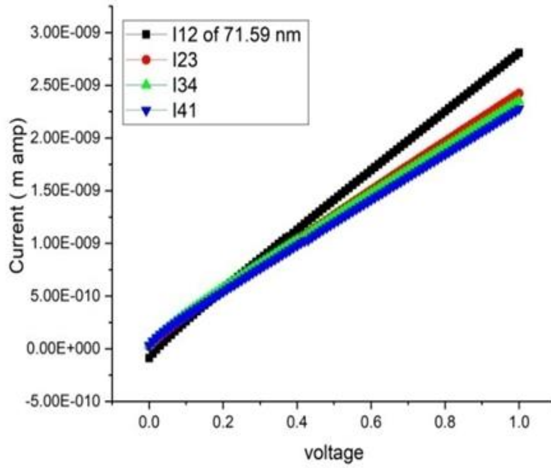

Figure 4: Sheet resistance of Ag_20 I-V curve (42 nm)

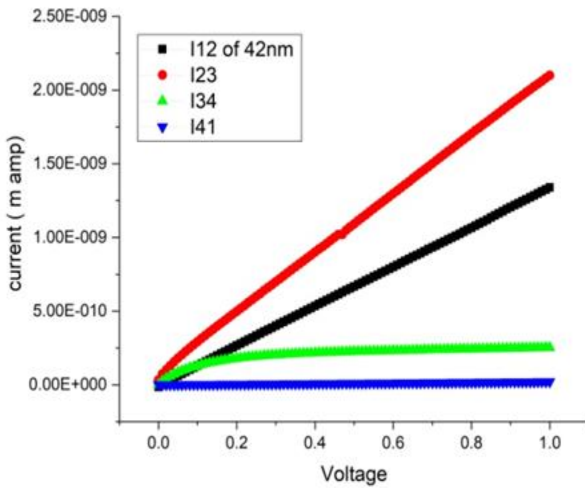

Figure 5: Sheet resistance of Ag_20 I-V curve (72 nm)

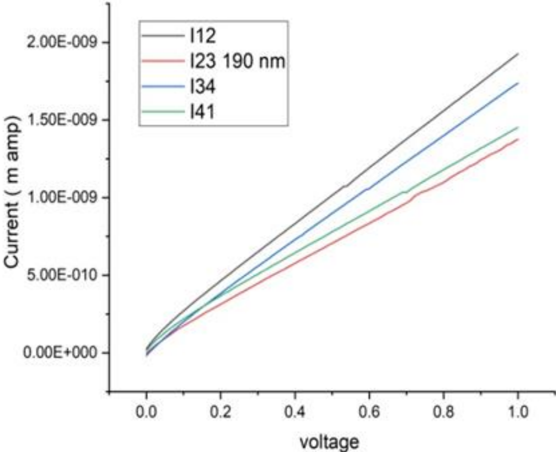

Figure 6: Sheet resistance of Ag_2O I-V curve (190 nm)

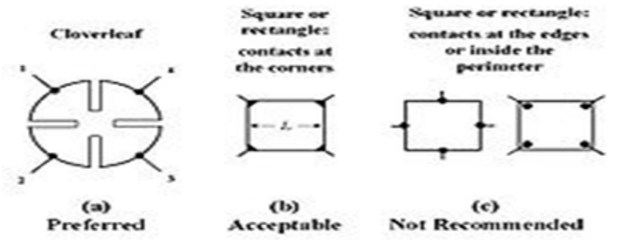

3.4. Resistivity analysis

The dependence of electrical resistivity on film thickness for silver oxide thin films is depicted in Fig.7. To accurately determine the resistivity, measurements were performed using the van der Pauw technique, which

is a widely accepted four-probe method for characterising thin films with arbitrary geometry. Resistivity (ρ) has been calculated using the Van der Pauw equation:

ρ=πdln (2) · (VI)\rho = \frac{\pi d}{\ln (2)} \cdot \left(\frac{V}{I} \right)

ρ=ln (2) πd· (IV)

Where:

- Film thickness is d,
- Voltage is measured in V
- The applied current is I, and
- VI\frac {V}{I}, I V gives the sheet resistance.

Table1: Film thickness, Sheet resistance, resistivity and Error of the Ag_2O thin films.

S N	Film thickness (nm)	Sheet resistance (Ω/sq)	Resistivity (Ωxm)	Error
1	42	7.90×10^{8}	3.32×10^{3}	± 240
2	72	4.53×10^{8}	2.62×10^{3}	± 200
3	190	9.50×10^{7}	1.81×10^{3}	± 158
4	326	6.80×10^{7}	2.29×10^{3}	± 310

According to reported research studies on silver oxide thin films, the variation of resistivity with thickness shows a non-linear trend. At lower thickness, high resistivity is commonly attributed to discontinuous island growth, where limited grain connectivity and strong surface scattering dominate charge transport. As thickness increases, the film becomes more continuous and compact, leading to improved crystallinity and reduced grain boundary scattering, which lowers resistivity.

Several studies on RF-sputtered silver oxide films report a minimum resistivity at intermediate thickness due to optimal microstructural properties, such as a larger grain size and reduced defects. However, at higher thickness, an increase in resistivity is often observed. This is due to many factors, such as oxygen non-stoichiometry, defect formation, and structural disorder. Additionally, phase instability in silver oxide films can lead to the formation of metallic Ag or mixed oxide phases, disrupting uniform conduction pathways.

Research articles also highlight that sputtering conditions, including oxygen partial pressure and deposition rate, strongly influence this behaviour. Thus, a similar trend of increasing resistivity with thickness has been reported for Unconventional thickness dependence of electrical resistivity of silver film electrodes in sub-stoichiometric oxidation states [17].

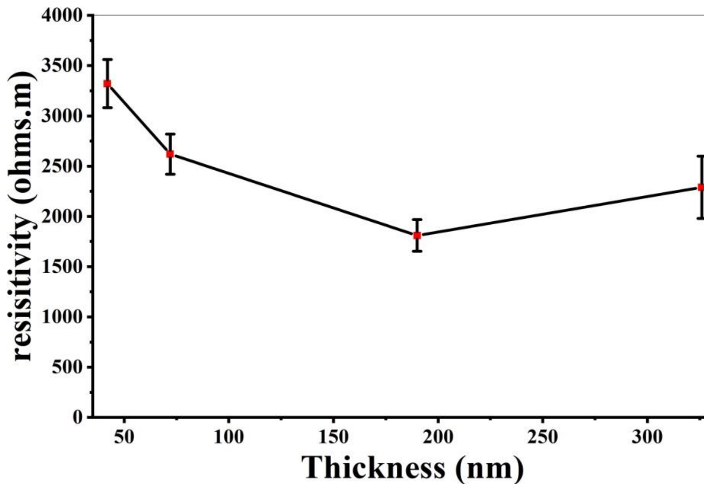

Figure 7: Electrical resistivity versus thickness of Silver Oxide thin films

3.5. X-ray diffraction (XRD) studies for structural analysis

To evaluate the crystallographic structure and phase purity of the silver oxide thin films, X ray diffraction (XRD) analysis was performed on samples deposited at varying deposition times of 3,5, 7 and 9 minutes, respectively. Fig.8 (a) displays the resultant XRD patterns. The diffraction patterns exhibit prominent Bragg reflections at approximately $26.65°, 33.87°, 38.28°, 44.00°$and $54.70°$, which correspond to the crystallographic planes (110) $(111), (200)$, $(211)$and(220) of cubic silver oxide respectively. These peaks are in good agreement with the standard JCPDS file No. 00-001-1041, confirming the successful formation of crystalline silver (I) oxide (Ag_2O) on the FTO substrates.

In addition to the primary silver oxide peaks, additional reflections are seen at roughly $26.65°, 37.95°, and\ 51.76°$, corresponding to the $(110), (200),$ and(211) planes of tin oxide, which originate from the underlying FTO (fluorine-doped tin oxide) substrate. These reference peaks much with JCPDS file no. 00-041-1445 and serve as substrate signatures rather than interference.

Among these reflections, the (200) peak around 38° appears as the most intense, indicating a preferred orientation along these crystallographic planes. Importantly, no additional peaks corresponding to metallic silver or other oxide phases are detected, suggesting the formation of a phase-pure Ag_2O structure.

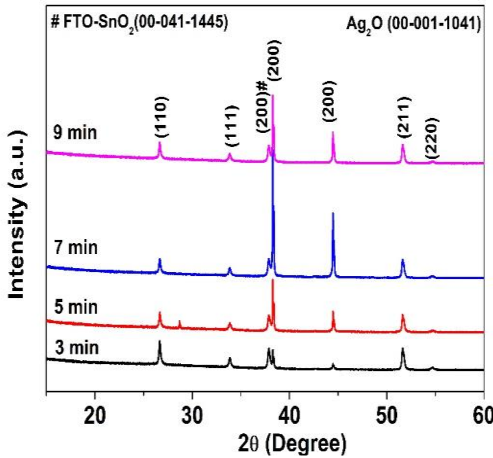

Figure 8: XRD of Ag_2O thin films Intensity (a.u) Vs 2θ (Degree).

A clear trend is observed in the relative intensity of the silver oxide diffraction peaks with increasing deposition time. The sample deposited for 3 minutes displays the lowest intensity, indicating lower crystallinity or a thinner film. In contrast, the samples deposited for 5, 7, and 9 minutes show progressively stronger diffraction peaks, reflecting enhanced crystallinity and greater phase formation due to longer deposition durations. Additionally, a slight shift in the Bragg angles with increasing deposition time is evident in the diffraction peaks in Fig. 8(a). This shift may be attributed to lattice strain, variation in crystallite size, or the proffered orientation resulting from increased film thickness and energy accumulation during sputtering.

To further qualify the crystalline nature of the silver oxide films, the average crystallite size (D) was calculated using the Debye-Scherrer equation.

$$D = \frac{K\lambda}{\beta \cos \theta} \tag{1}$$

Where:

D is the crystalline size,

Shape factor is K (usually 0.9),

(λ) is the X-ray wavelength (CuK_{α} = 1.5406 Å).

Beta (β) is the full width at half maximum (FWHM) of the diffraction peak (in radians).

The Bragg angle is Theta (θ).

Phase	**3 min**		**5 min**		**7min**		**9min**	
	2θ	FWHM	2θ	FWHM	2θ	FWHM	2θ	FWHM
Ag_2O	26.6558	0.118	6.6789	0.039	26.6613	0.108	26.652190	0.049
	33.8949	0.048	33.8731	0.168	33.8261	0.118	33.827470	0.138
	38.2826	0.048	38.3939	0.048	38.3846	0.048	38.278930	0.060
	44.4608	0.048	44.5872	0.048	44.5797	0.048	44.575500	0.072
	54.7098	0.240	54.6722	0.240	54.6180	0.288	54.659550	0.288
FTO-SnO_2	26.6558	0.118	26.6270	0.059	26.6613	0.108	26.652190	0.049
	37.8308	0.036	37.8360	0.048	37.8199	0.049	37.850630	0.039
	51.7642	0.096	51.7857	0.120	51.7531	0.120	51.769070	0.096

The crystallite sizes ranged from 44.68 nm to 53.07 nm, increasing with deposition time, consistent with increased grain growth and improved crystallinity. In addition, structural parameters such as interplanar spacing (d) and lattice constant (a) for the cubic phase of silver oxide were also calculated using Bragg's law and appropriate crystallographic relations. The estimated values are presented in Table 2 and are in concordance with literature–reported data [18-19], further validating the structural integrity of the synthesized thin films.

Table2: Lattice parameters of **Silver Oxide** samples with different deposition time.

S.N.	**Sample**	**3min**	**5min**	**7min**	**9min**
1	d (Å)	2.644	2.644	2.648	2.647
2	a (Å)	4.580	4.580	4.586	4.585
3	D (nm)	44.71	45.12	53.07	44.68

3.6. The surface morphology analysis by FESEM

The surface morphology of silver oxide thin film has been measured using FESEM. Fig. 9 and 10 show the micrographs of films with thicknesses of 42 nm and 72 nm, respectively. Prior to imaging, the sample has been annealed at 200° C for 2 hours to enhance crystallinity and reduce surface defects introduced during sputtering. Both films exhibit agglomerated granular structures with irregularly shaped grains randomly distributed across the surface. The broad size distribution observed is characteristic of sputter-deposited oxide films subjected to post-annealing, where grain growth and coalescence of smaller crystallites occur. A clear dependence of grain size on film thickness is evident: The 42 nm films (Fig.9) display relatively fine grains, whereas the 72 nm films (Fig.10) show the larger, more densely packed granules. This indicates enhanced grain growth with increased deposition time and material accumulation. This agglomerated morphology likely arises from surface energy minimisation during nucleation and growth, leading to grain clustering. This trend is consistent with earlier reports on sputtered silver oxide thin films [20-21]. Such morphological evolution directly affects film properties: larger grains typically reduce grain boundary density and scattering, thereby improving electrical conductivity and influencing optical characteristics. FESEM result complements the structural and electrical analysis, highlighting the combined effects of thickness and annealing on the morphology and performance of silver oxide thin films.

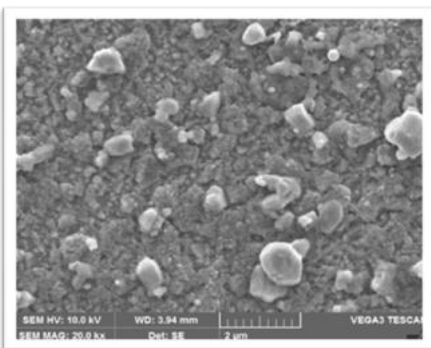

Figure 9: FESEM of 42nm Ag_2O at 20 k

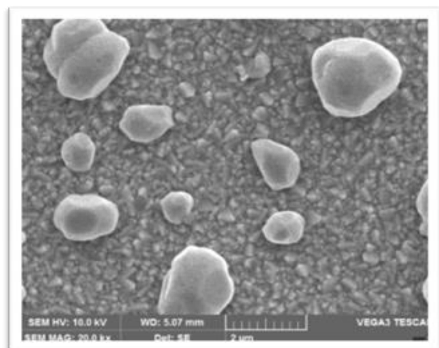

Figure 10: FESEM of 72 nm Ag_2O at 20 k

4. Conclusion

1. Silver oxide nano films have been effectively deposited on FTO glass substrates applying RF sputtering technique.

2. Film thickness, which ranges from 42-660nm, was accurately determined using a non- contact optical profiler, confirming uniform deposition across the substrates.
3. Electrical resistance analysis was carried out by using the Vander Pauw technique, and corresponding current-voltage (I-V) curves have been plotted to assess the electrical behaviour of films.
4. The resistivity of silver oxide thin films decreases with increasing thickness due to improved continuity and reduced scattering, reaching a minimum at ~190 nm ±
5. XRD studies confirmed the crystalline nature of silver oxide (Ag_2O) films, with diffraction peaks corresponding to standard Ag_2O phases. Increasing deposition time enhanced crystalinity and peak intensity.
6. FESEM analysis revealed the formation of nanostructured, agglomerated grains, with grain size increasing with film thickness. The surface morphology was irregular, indicating the presence of nanoparticles with undefined geometry.

Generally, present research describes that film thickness significantly influences the structural, morphological, and electrical characteristics of Silver Oxide thin films. These findings provide valuable insights for optimising Silver Oxide films in applications such as sensors, photovoltaics, and other electronic devices.

Future scope

Silver oxide thin films have attracted significant attention, especially when deposited on FTO glass substrates. Band gap of Ag_2O ranges from 1.2 to 3.4 eV; its notable optical and electrical characteristics make it a promising candidate for application in photovoltaics, photo-catalysis, sensors, medical fields and rechargeable batteries, etc.

Acknowledgement

I express my sincere gratitude to Dr. H. C Nagraj, Mrs. Veena and Mr. Killari Naveen Kumar of "NITTE Meenakshi institute of technology" for their constant support and valuable assistance in preparation and characterization of the silver oxide thin films samples.

Author contribution

Shivakumar Siddanna has done experimental work, Devidas. G. B has given technical support and monitored on the experimental work mean while Omnath Patil helped in the technical analysis of the experimental

results and S.M. Hanagodimath has monitored the overall work, gone through the manuscript. The manuscript preparation by the first author and all authors has been read and approved.

Funding

We have not received any funding from UGC or Government agencies.

References

[1]. N. R. C. Raju, K. J. Kumar, and A. Subrahmanyam, "Physical properties of silver oxide thin films by pulsed laser deposition: Effect of oxygen pressure during growth," *J. Phys. D, Appl. Phys.*, vol. 42, no. 13, p. 135411, 2009.

[2]. N. T. Tsendzughul and A. A. Ogwu, "Visible light activated antimicrobial silver oxide thin films," in *Advances in Medical and Surgical Engineering*, W. Ahmed, D. A. Phoenix, M. J. Jackson, and C. P. Charalambous, Eds. London, UK: Academic Press, 2020, pp. 179–239, doi: 10.1016/B978-0-12-819712-7.00012-7.

[3]. S. Siddanna, G. B. Devidas, B. S. Nischit, K. Naveenkumar, and S. M. Hanagodimath, "Optical Studies of Silver Oxide Deposited Thin Films Using the RF Sputtering Technique," *Indian J. Sci. Technol.*, vol. 17, no. 40, pp. 4138–4143, Oct. 2024, doi: 10.17485/IJST/v17i40.1079.

[4]. S. R. Lee, M. M. Rahman, K. Sawada, and M. Ishida, "Fabrication of a highly sensitive penicillin sensor based on charge transfer techniques," *Biosens. Bioelectron.*, vol. 24, no. 7, pp. 1877–1882, 2009.

[5]. A. Díaz-Parralejo, R. Caruso, A. L. Ortiz, and F. Guiberteau, "Densification and porosity evaluation of ZrO_2–3 mol.% Y_2O_3 sol–gel thin films," *Thin Solid Films*, vol. 458, no. 1–2, pp. 92–97, 2004.

[6]. S. R. Lee, M. M. Rahman, M. Ishida, and K. Sawada, "Development of a highly-sensitive acetylcholine sensor using a charge-transfer technique on a smart biochip," *TrAC, Trends Anal. Chem.*, vol. 28, no. 2, pp. 196–203, 2009.

[7]. G. A. Mostafa and A. Al-Majed, "Characteristics of new composite- and classical potentiometric sensors for the determination of pioglitazone in some pharmaceutical formulations," *J. Pharm. Biomed. Anal.*, vol. 48, no. 1, pp. 57–61, 2008.

[8]. C. Feldmann and H. O. Jungk, "Polyol-mediated preparation of nanoscale oxide particles," *Angew. Chem. Int. Ed.*, vol. 40, no. 2, pp. 359–362, 2001.

[9]. L. J. Van der Pauw, “A method of measuring specific resistivity and Hall effect of discs of arbitrary shape,” *Philips Res. Rep.*, vol. 13, no. 1, pp. 1–9, 1958.

[10]. W. G. John, *Measurement, Instrumentation and Sensors*. New York, NY, USA: McGraw-Hill, 1998.

[11]. W. B. Elsharkawy *et al.*, “Tuning the structural, optical properties and antibacterial activity of poly (vinyl chloride)/poly (methyl methacrylate)/silver oxide nanocomposites for potential optoelectronic and medical applications,” *Sci. Rep.*, vol. 15, no. 1, p. 41722, 2025.

[12]. K. N. Kumar *et al.*, “Sputter deposited tungsten oxide thin films and nanopillars: Electrochromic perspective,” *Mater. Chem. Phys.*, vol. 278, Art. no. 125706, 2022, doi: 10.1016/j.matchemphys.2022.125706.

[13]. J. Gupta, H. Shaik, K. N. Kumar, S. A. Sattar, and G. A. Reddy, “Optimization of deposition rate for E-beam fabricated tungsten oxide thin films towards profound electrochromic applications,” *Appl. Phys. A*, vol. 128, no. 6, p. 498, 2022.

[14]. M. A. Dawood *et al.*, “Some of electrical and detection properties of nano silver oxide,” in *IOP Conf. Ser.: Mater. Sci. Eng.*, vol. 454, no. 1, p. 012161, 2018.

[15]. A. Purohit, S. Chander, A. Sharma, S. P. Nehra, and M. S. Dhaka, “Impact of low temperature annealing on structural, optical, electrical and morphological properties of ZnO thin films grown by RF sputtering for photovoltaic applications,” *Opt. Mater.*, vol. 49, pp. 51–58, 2015.

[16]. R. Karthick *et al.*, “Understanding the enhanced electrical properties of free-standing graphene paper: The synergistic effect of iodide adsorption into graphene,” *RSC Adv.*, vol. 9, no. 58, pp. 33781–33788, 2019.

[17]. J. Yun *et al.*, “Unconventional thickness dependence of electrical resistivity of silver film electrodes in substoichiometric oxidation states,” *Acta Mater.*, vol. 265, p. 119637, Feb. 2024, doi: 10.1016/j.actamat.2023.119637.

[18]. S. F. Alhasan, B. A. Bader, and E. T. Salim, “Surface morphology and roughness of silver oxide prepared employing pulsed laser at optimum laser fluence,” *Mater. Today: Proc.*, vol. 42, pp. 2845–2848, 2021.

[19]. A. V. Filip *et al.*, “Ultrathin films of silver by Magnetron Sputtering,” *Inorganics*, vol. 10, no. 12, Art. no. 235, 2022, doi: 10.3390/inorganics10120235.

[20]. S. Sagadevan, “Synthesis, structural, surface morphology, optical and electrical properties of silver oxide nanoparticles,” *Int. J. Nanoelectron. Mater.*, vol. 9, no. 1, pp. 1–7, 2016.

[21]. S. Asgary and P. Esmaili, “Effect of reactive gas flow on structural and optical properties of sputtered silver oxide thin films; Kramers–Kronig method,” *Opt. Quantum Electron.*, vol. 55, no. 2, Art. no. 118, 2023, doi: 10.1007/s11082-022-04388-y.